Morphology and spacing of river meander scrolls

Strick, Robert J. P.; Ashworth, Philip J.; Awcock, Graeme; Lewin, John

Published in:
Geomorphology

DOI:
10.1016/j.geomorph.2018.03.005

Publication date:
2018

Citation for published version (APA):
Strick, R. J. P., Ashworth, P. J., Awcock, G., & Lewin, J. (2018). Morphology and spacing of river meander scrolls. *Geomorphology*, *310*, 57-68. https://doi.org/10.1016/j.geomorph.2018.03.005

Geomorphology 310 (2018) 57–68

Contents lists available at ScienceDirect

Geomorphology

journal homepage: www.elsevier.com/locate/geomorph

Morphology and spacing of river meander scrolls

Robert J.P. Strick [a,*], Philip J. Ashworth [a], Graeme Awcock [a], John Lewin [b]

[a] Division of Geography and Geology, School of Environment and Technology, University of Brighton, Lewes Road, Brighton BN2 4GJ, UK
[b] Department of Geography and Earth Sciences, Aberystwyth University, Llandinam Building, Penglais, Aberystwyth SY23 3DB, UK

ARTICLE INFO

Article history:
Received 15 November 2017
Received in revised form 6 March 2018
Accepted 7 March 2018
Available online 9 March 2018

Keywords:
Point bars
Scroll spacing
Meander bends
Mississippi River

ABSTRACT

Many of the world's alluvial rivers are characterised by single or multiple channels that are often sinuous and that migrate to produce a mosaicked floodplain landscape of truncated scroll (or point) bars. Surprisingly little is known about the morphology and geometry of scroll bars despite increasing interest from hydrocarbon geoscientists working with ancient large meandering river deposits. This paper uses remote sensing imagery, LiDAR data-sets of meandering scroll bar topography, and global coverage elevation data to quantify scroll bar geometry, anatomy, relief, and spacing. The analysis focuses on preserved scroll bars in the Mississippi River (USA) floodplain but also compares attributes to 19 rivers of different scale and depositional environments from around the world.

Analysis of 10 large scroll bars (median area = 25 km^2) on the Mississippi shows that the point bar deposits can be categorised into three different geomorphological units of increasing scale: individual 'scrolls', 'depositional packages', and 'point bar complexes'. Scroll heights and curvatures are greatest near the modern channel and at the terminating boundaries of different depositional packages, confirming the importance of the formative main channel on subsequent scroll bar relief and shape. Fourier analysis shows a periodic variation in signal (scroll bar height) with an average period (spacing) of 167 m (range 150–190 m) for the Mississippi point bars. For other rivers, a strong relationship exists between the period of scroll bars and the adjacent primary channel width for a range of rivers from 55 to 2042 mis ~50% of the main channel width. The strength of this correlation over nearly two orders of magnitude of channel size indicates a scale independence of scroll bar spacing and suggests a strong link between channel migration and scroll bar construction with apparent regularities despite different flow regimes. This investigation of meandering river dynamics and floodplain patterns shows that it is possible to develop a suite of metrics that describe scroll bar morphology and geometry that can be valuable to geoscientists predicting the heterogeneity of subsurface meandering deposits.

1. Introduction

Alluvial floodplains, and in particular those associated with the world's largest rivers, have a complex relief (Rozo et al., 2012; Lewin and Ashworth, 2014a; Latrubesse, 2015) that is produced by recurring erosional, and depositional events (Day et al., 2008). The magnitude, heterogeneity, spatial distribution, and connectivity of this relief controls river floodwater routing and storage, sediment dispersal, and biogeochemical cycling (Mertes, 1997; Hess et al., 2003; Aufdenkampe et al., 2011; Lewin and Ashworth, 2014b). However, because many river floodplains are inaccessible, and in the world's largest rivers are often densely vegetated (e.g., Trigg et al., 2012, 2014; O'Loughlin et al., 2013), it is especially challenging to characterise and quantify the morphology, geometry, and topography of floodplain relief. Yet such metrics are important for defining habitat structure, flood hazard mapping, and isolating zones for preferential accumulation of fine-grained sediment, organics, and contaminants.

The world's largest rivers, defined here as having an annual average discharge >1000 m^3/s (Latrubesse, 2008), are characterised by anabranching channel patterns (Ashworth and Lewin, 2012; Carling et al., 2013) with multiple channels that are often highly sinuous, and by floodplains that are dominated by back-to-back and truncated scrolls (e.g., Mertes et al., 1996; Rozo et al., 2012). Some, like the Mississippi River (Saucier, 1994) and many smaller ones, are predominantly meandering. Point bars are usually produced by river lateral migration causing concomitant outer-bend bank erosion and corresponding inner-bend deposition to produce a series of undulating 'ridges' and 'swales' or scrolls (Hickin and Nanson, 1975; Hooke and Harvey, 1983; see Fig. 1).

Although much work has been undertaken on the underlying processes and principles that govern meander shape (e.g., Lanzoni and Seminara, 2006; Hooke, 2007; Lazarus and Constantine, 2013; Vermeulen et al., 2016), surprisingly little research has focused on the product of meander bend migration. It is widely acknowledged that scroll bars dominate portions of the floodplains along rivers, but even

* Corresponding author.
E-mail address: R.J.Strick@brighton.ac.uk (R.J.P. Strick).

https://doi.org/10.1016/j.geomorph.2018.03.005

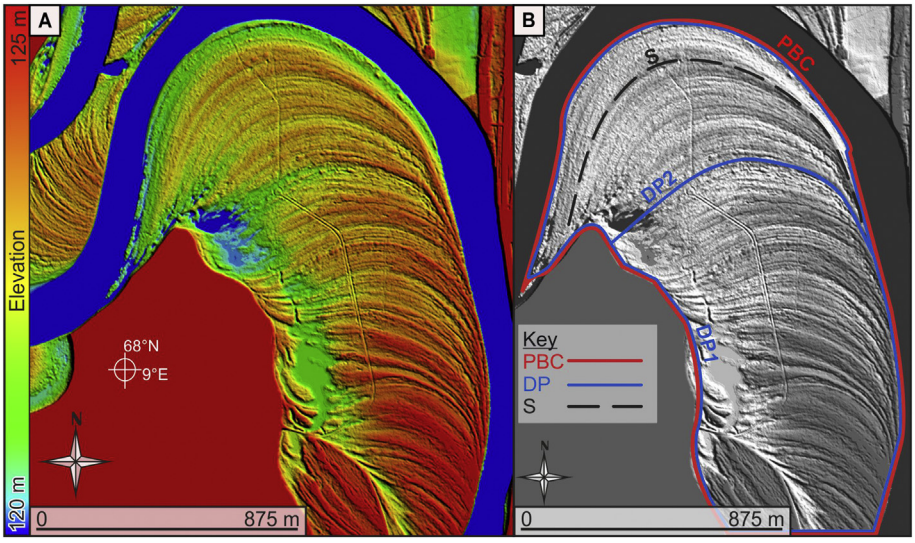

Fig. 1. (A) LiDAR DEM from the Ivalojoki River, Finland (National Land Survey of Finland Topographic Database 06/2015); elevations above 125 m have been cropped to show better the internal scroll bar topographic variation. (B) Hierarchy of scroll bar forms as detailed in Table 1: a point bar complex (PBC), depositional packages (DP), and a scroll (S).

some basic questions about their formation and topography are unresolved. For example, are individual scrolls spaced a regular distance apart, what controls this spacing, is there a characteristic morphology for scrolls, and what happens to scroll spacing and morphology at the edges of different and discrete depositional packages?

Pioneering work on meander bend dynamics and point bar formation was conducted on the gravel-bed Beatton River, Canada (Hickin and Nanson, 1975). Nanson (1980) further described scroll bar morphology as well as detailing meander dynamics, together with specifications for elevations and grain sizes along two particular scrolls of the Beatton River. Some experimental modelling of scroll bar formation and meander bend migration (e.g., Peakall et al., 2007; Parker et al., 2011; van Dijk et al., 2013; van de Lageweg et al., 2014; Schwenk et al., 2015); but despite reproducing realistic planform morphologies, these experimental models still tend to be analogue only (i.e., not Froude-scaled models) and may not be truly representative of larger rivers that have predominately sandy beds. Significant progress has been made in the numerical simulation of river meander evolution since the pioneering work of Ikeda et al. (1981), aided by rapid increases in computational power (e.g., Sun et al., 1996; Zolezzi and Seminara, 2001; Chen and Duan, 2006; Blanckaert and de Vriend, 2010). However, progress is still needed to numerically replicate the natural evolution processes of meandering channels, because of strong nonlinear interactions (Gu et al., 2016). More recently, van de Lageweg et al. (2014) proposed that river channel width is instrumental in the formational dynamics of scroll bars, with erosional enlargement at the outer bank (bank pull) driving the process for deposition.

What needs to be added from this previous research is a robust quantification of the geometry and morphology of a range of different types and scales of scroll bar. This paper uses remote sensing imagery, of mostly large rivers, with a particular focus on the Mississippi River. We use statistical analysis of data-sets derived from remotely sensed multispectral imagery, light detection and ranging (LiDAR), shuttle radar topography mission (SRTM), and advanced spaceborne thermal emission and reflection radiometer (ASTER) data-sets with the specific objectives of:

- developing new metrics that describe the nature of and different scales of topography and floodplain relief involving meander scrolls and associated overbank infills on large river floodplains;
- quantifying and classifying meander point bar complexities, including scroll periodicities, distributions of scrolls, and package formations for the Mississippi River; and
- extending the analysis undertaken on the Mississippi to 19 contrasting rivers in different climatic settings to test scale independence of the results and variability across different biomes.

2. The Lower Mississippi River

The Mississippi River is the tenth largest river in the World (Gupta, 2007) with a predominantly meandering channel pattern and extensive sets of preserved scrolls in the contemporary channel and adjacent floodplain. The present geomorphology of the Lower Mississippi River has been modified by artificial channel improvements: meander cutoffs, levee construction, diversion structures, stabilization of channel banks, and river training dikes (Biedenharn and Thorne, 1994; Knox and Laturbesse, 2016). The construction of significant levees has minimised floodplain inundation by constraining much of the flood water within the channel, allowing for the preservation of scroll bar forms on the extended floodplain.

The river drains a basin of ~3,224,600 km^2 that represents about 41% of the 48 contiguous United States and a small area of two Canadian provinces (Knox, 2007). The valley floor boundary to the west is not easy to define, because the merging of adjacent valleys of some principal tributaries with the main Mississippi valley (Harmar and Clifford, 2006). The current course of the Lower Mississippi River partly follows an easterly bluff line (Fig. 2A), apart from between Memphis and Vicksburg where it flows across the central alluvial valley leaving an extensive set of palaeochannels and scrolls (Knox, 2007; Fig. 2A). Saucier (1994) suggests that the Mississippi has followed its present course for ~2000 years, despite repeated cycles of meander bend growth and cutoff.

There are two large geologic uplift features within the Lower Mississippi valley: the Lake County Uplift and the larger Monroe Uplift (see Fig. 2A) (Harmar and Clifford, 2006). The alluvial architecture of the Holocene Lower Mississippi transitions in character down valley. Systematic mapping from Fisk (1947, 1944) and Saucier (1994) recognised that the Holocene floodplain upstream in the Yazoo basin (see Fig. 2A) has former channel belts up to 25 km wide. By contrast, the valley downstream is characterised by large floodplain basins bordering a comparatively narrow channel belt 5–10 km in width (Gouw and Autin, 2008). Six distinct meander belts have been identified (Knox, 2007; Fig. 2A), each extending up to hundreds of kilometres in length (Autin et al., 1991).

The reach of the Mississippi River used in this study lies in the states of Louisiana and Mississippi, between Vicksburg and Baton Rouge. The

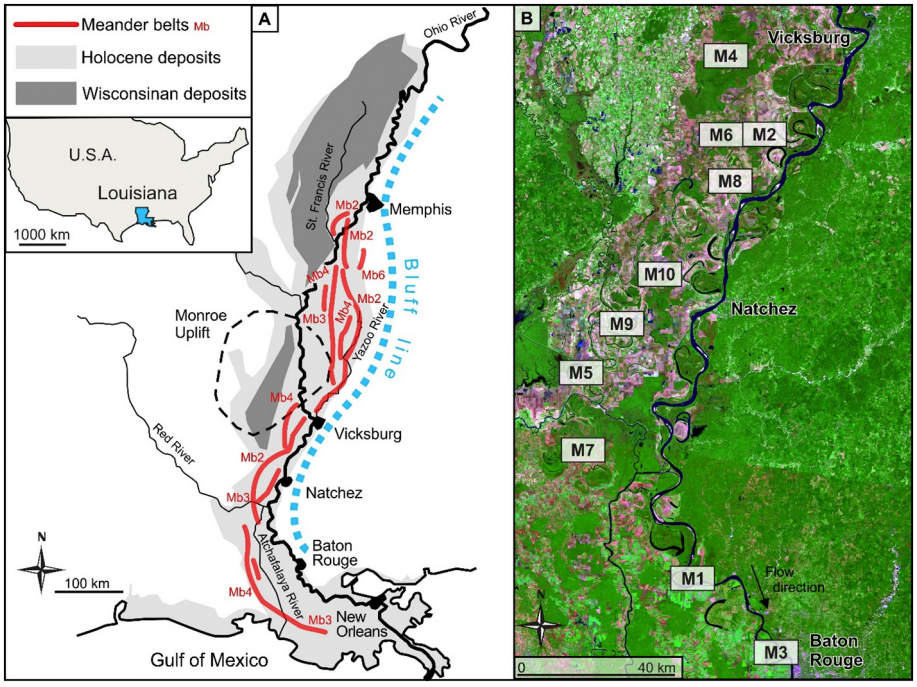

Fig. 2. (A) The Lower Mississippi River, including previous meander belts (map adapted from Knox, 2007). (B) False colour Landsat 8 satellite image (2013) of study location, showing the 10 meander bend study sites. Note that all sites are either located on or to the west of the river because of the high bluff on the eastern edge of the river.
Satellite data provided by the USGS.

study reach incorporates the entire floodplain, regardless of whether it is hydrologically connected during extreme events or not. Fig. 2B shows the locations of the 10 meander bends chosen for this investigation. The different bends represent an assortment of morphologies and current hydrological connectivity and ages.

3. Methods

Within each meander bend we identified a hierarchy of forms that characterise larger river meander deposits: idividual scrolls (S), depositional packages (DP) and point bar complexes (PBCs) as defined in Table 1 (see also Fig. 1).

A set of quantitative parameters for scroll bar measurements was devised. These are described and defined in Table 2 and illustrated in Fig. 3.

3.1. Interpolation and normalisation of scroll measurements

An interpolation technique was used in association with scroll bar measurements to reveal the spatial variability of the data. Height measurements were taken at five points along each scroll bar (see Table 2 and Fig. 3) and then interpolated using Universal Kriging. This is an advanced geostatistical method that produces an estimated surface from point cloud data. It was necessary to normalise the data-set per the dynamic range (so that each maximum becomes 1 and each minimum becomes 0) at each meander bend to facilitate comparison across the full range of sizes of meander bends investigated. The range of each meander bend data set was used to normalise the height, width, and curvature information for each bend, as shown in Eq. (1):

$$X_{norm} = \frac{X - X_{min}}{X_{max} - X_{min}} \quad (1)$$

where X_{norm} = normalised value, X = data point, X_{min} = minimum value in data range, X_{max} = maximum value in data range.

3.2. Spatial frequency analysis of scroll bar spacing using Fourier analysis

Fourier analysis of the height signal was used to test the hypothesis that scrolls have a characteristic spatial frequency. 'Spatial frequency' describes the periodic variation of signal amplitude (e.g. height) with distance such that the power of Fourier analysis can be used to explore periodicity in such signals. If a topographic feature occurs at regular intervals, there is a characteristic spatial frequency associated with it, which in terms of the spatial frequency power spectrum produced by a Fourier transform will be expressed as a peak in the amplitude. The more dominant the spatial frequency, the greater the amplitude peak shown in the Fourier transform (Fig. 4). In this study, a Fourier

Table 1
Classification and description of point bar elements with examples of previous work.

Scroll bar geomorphology	**Symbol**	Description	Examples of previous work
Scroll	S	Individual ridges on a floodplain surface, associated with the growth of a meander bend	Happ et al. (1940); Fisk (1944, 1947); Leopold et al. (1964); Allen (1965); Hickin (1974); Jackson (1976); Nanson (1980); Leclerc and Hickin (1997); Rodnight et al. (2005); Parker et al. (2007, 2011); van de Lageweg et al. (2014); Pietsch et al. (2015)
Depositional package	DP	Distinct packages of scrolls contained within a PBC	Nardin et al. (2013); Moreton and Carter (2015); Ghinassi et al. (2016); Durkin et al. (2017)
Point bar complex	PBC	A collection of scrolls associated with a meander bend	Hickin (1974); Nardin et al. (2013); Durkin et al. (2015); Moreton and Carter (2015); Ghinassi et al. (2016); van de Lageweg et al. (2014); Martinius et al. (2017); Durkin et al. (2017)

Table 2
Euclidean geometry measurement criteria for scroll bar topography (see also Fig. 3).

Measurement or parameter	Description
Distance from channel	A line is drawn between the two points of bend inflection (A-A′; in plan). From the middle of A′ a perpendicular line is drawn (B-B′), out to the river channel. Each scroll is measured where it crosses B-B' and assigned a unique 'Scroll number' used as an index for all other measurements, as labelled on Fig. 3A. If a scroll does not dissect the line its position is measured relative to the line. These measurements are the red lines and annotations in Fig. 3A.
Span	Confined by the scroll packages as highlighted by the different colours in Fig. 3A and by the river channel. Truncation of the scroll by the package boundary dictates where the scroll begins/ends.
Length	The straight distance of the scroll as depicted in Fig. 3A as the blue dashed line.
Width	Measured on the elevation profile at the centre/middle of the scroll as defined by the length. Width is measured from the inflection point of the swale (in elevation), over the ridge to the inflection point of the next swale; see Fig. 3A.
Height	Measured on the elevation profile at the same point as the width of the scroll. Height is the highest point of the scroll to the lowest point on the swale. The lowest point of the swale is an average from both sides of the scroll ridge; see Fig. 3B.
Height-to-width ratio (HW)	Height-to-width ratio is computed from the height measurements; see Fig. 3C.
Curvature	Span divided by length gives a measure for curvature of the scroll; see Fig. 3D.
River channel width	Deriving channel widths from aerial images can pose problems of subjective interpretation as riparian vegetation can obstruct channel banks, there are also differences at high and low flow (Luchi et al., 2010), and pixel resolution can reduce accuracy. Having topographic information is then very important to be able to identify clearly the river channel boundaries. Therefore, profiles are drawn across the river channel to establish the river banks. The width of the meander river channel is measured at five points along the channel at equal spacing relative to the meander bend length (length of bend measured and then divided by five to give the intervals of measurement); these lengths are then averaged to give a channel width for the whole bend. The example river channel widths are indicated by the green arrows in Fig. 3A.

transform was used to determine the spatial frequency spectra of data-sets describing scroll bar topography. The methodology has been developed using Mississippi LiDAR data (5-m resolution) as the source of topographic information (Sections 4.1–4.5). It was later applied in Section 4.5 to elevation data-sets from SRTM and ASTER data (30-m resolution) and other LiDAR data sources as referred to in Table 4.

To aid in the spatial frequency analysis, LiDAR data were transformed via Automatic Local Thresholding (ALT) (Landini, 2016). This is a process of automated binary 'segmentation'. Ridges are treated as binary 'foreground' (white) and the swales as binary 'background' (black). To make that binary conversion effective and yet meaningful, a method was sought that automatically decided an effective 'zero' level. This relates to a 'zero-crossing' concept, which in the context of scrolls is where the elevation values change from ridge to swale (Fig. 4A and B). Reliable differentiation was verified by comparing the binary image in Fig. 4B, where ridges are white and swales are black, with greyscale image of topographic variation in Fig. 4A, where ridges are brighter and swales are darker.

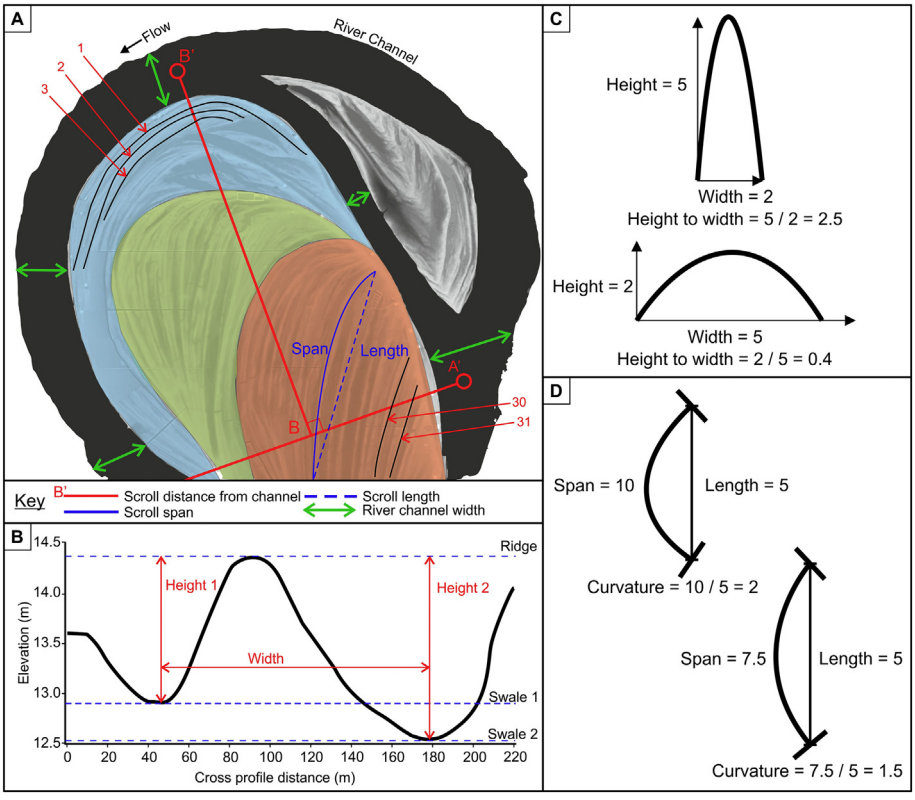

Fig. 3. (A) A point bar complex on the Mississippi River with the various measurement definitions. (B) A typical elevation profile showing how scroll height and widths are calculated. (C) Scroll height to width ratios and how this shape is represented with a scroll in profile view. (D) Different scroll curvature values in planview.

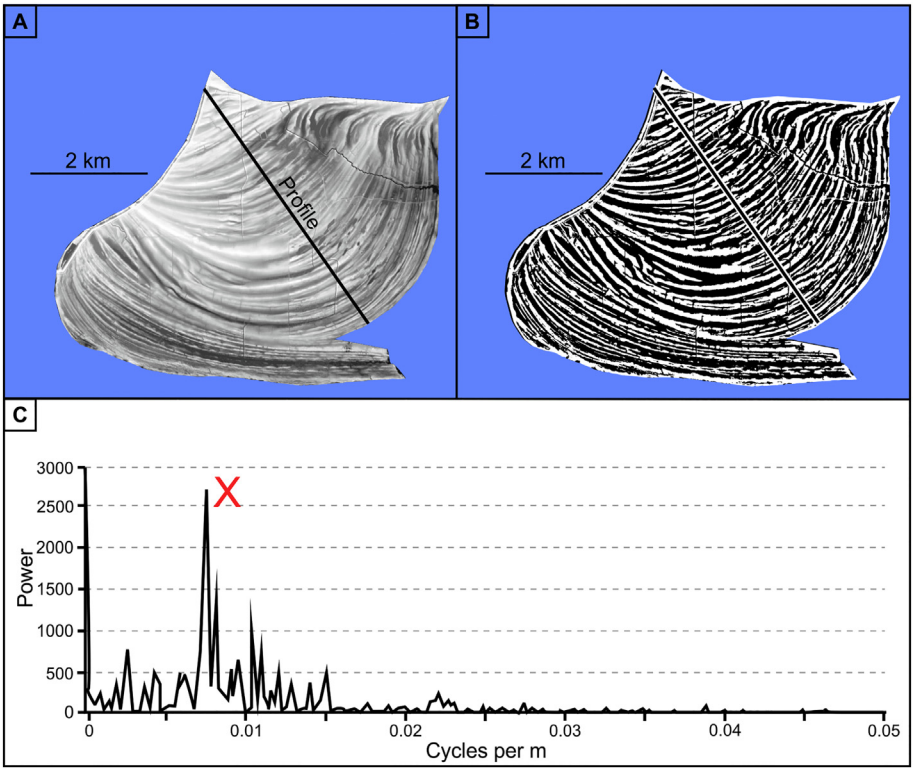

Fig. 4. (A) DEM of meander bend M9 derived from LiDAR (data from the Louisiana statewide LiDAR project); and (B) binary output from the Automatic Local Thresholding (ALT) segmentation process, where white (foreground) = ridge and black (foreground) = swale; (C) Frequency power spectrum derived from the binary profile A very distinct peak is visible in the data labelled 'X' (equal to a spacing of a scroll every 173 m).

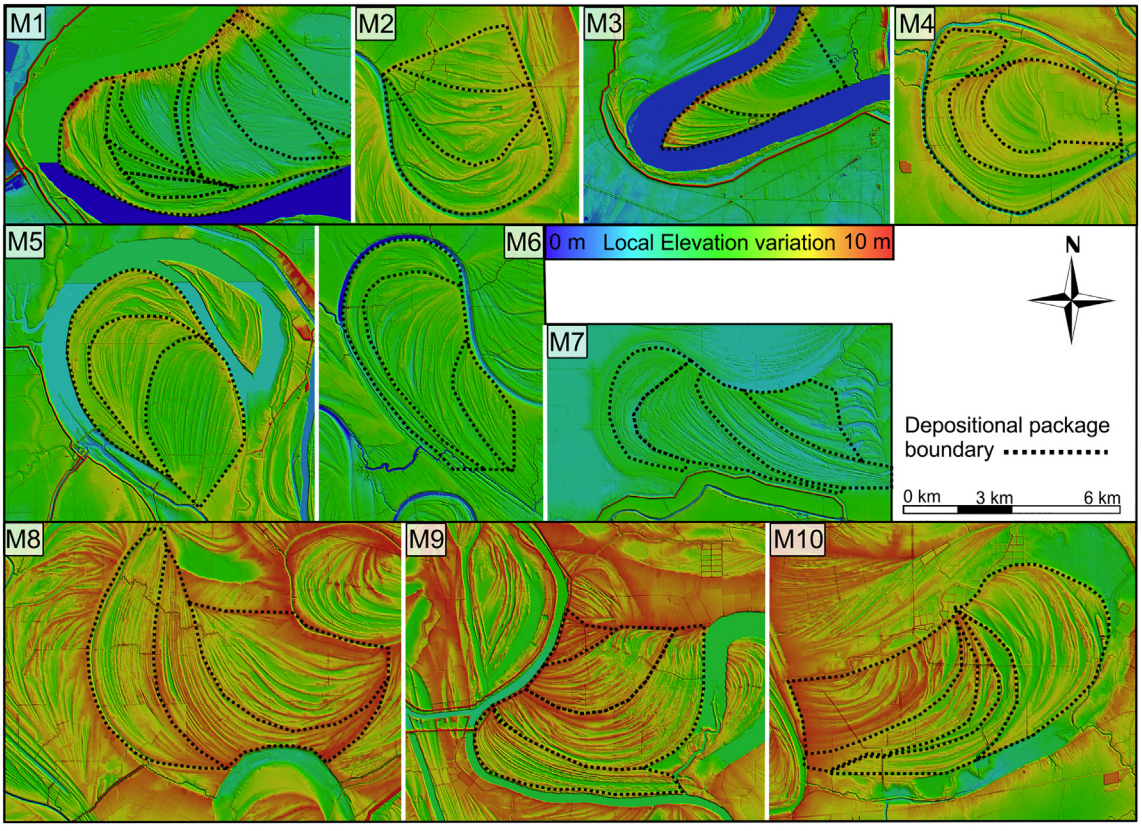

Fig. 5. Ten meander bends on the Mississippi River floodplain used in this study; all bends are plotted to the same elevation scale. See bend locations in Fig. 2. LiDAR bare-earth DEM information was sourced from the Louisiana State LiDAR project.

4. Results

4.1. Meander bends analysis

Data were collected from LiDAR-derived bare-earth DEMs provided by the U.S Geological Survey (USGS). Fig. 5 shows DEMs of meander bends M1 to M10, with the individual depositional packages highlighted by dashed lines. Only two of the ten bends are still connected to the present main channel at low flow, with the remaining only receiving water and sediment inputs from floodplain channels or during flood events. The two bends that are connected to the main channel (M1 and M3) do have extensive metre-scale artificial levees surrounding their outer banks, which is likely to reduce current channel migration and therefore scroll formation. The radius of curvature varies between bends together with the total number of individual scrolls (Table 3), relating to the different developmental ages of the bends; and bends show a range of shapes and sizes of depositional packages (Fig. 5).

4.2. Interpretation of scroll bar geomorphology

Fig. 6 shows summary information derived from profiles across each of the 10 meander bends. Heights of scrolls (Fig. 6A) have similar medians within a range of ±1 m. However, the quartiles and totals come within a 4-m range. This suggests that there may be a 'typical' height of a scroll for this reach of the Mississippi River, which is likely associated with adjustment to the mean annual flood or some other significant flood recurrence interval. However, each bend displays internal scroll height heterogeneity within it. No clear relationship exists between the heterogeneity of scroll heights and meander bend geometry (Table 2). Larger bends do not necessarily have greater ranges and sizes of scrolls, and there is no clear relationship between current radius of curvature and scroll height.

The widths of scrolls (Fig. 6B) show a similar trend, with ranges, quartiles, and medians. Meander bends M1 and M10, however, are dissimilar and have much larger scroll widths within the PBC, particularly M10. The widths of M10 may be much larger because of the rotational migration of the associated channel (Fig. 5), the rotation of the point bar stretches the width of the scroll as it rotates back on its self. Fig. 7A shows the relationship of scroll widths to the width of the adjacent river channel ($R^2 = 0.57$; p value = 0.097). In cases with no clear channel remnant, the present average channel width was used as a proxy measurement. Fig. 7B shows how average scroll width relates to the adjacent river channel width. The results show that the width of scrolls is equivalent to around 15 to 25% of the river channel, as

Table 3
Morphological attributes of the 10 meander bends and their hydrological connectivity; the rc/w_m is the radius of channel curvature to mean channel width (note, the mean river channel width of 678 m is used when no distinctive preserved river channel is present adjacent to the bend and is highlighted in bold).

Meander bend	Total area (km^2)	Radius of curvature of channel (rc km)	Channel width (W m)	rc/w_m	Number of scrolls	Hydrological connectivity
M1	32.7	2.3	815	2.8	61	Main-stem
M2	18.4	2.6	**678**	3.8	24	Partial
M3	9.6	1.2	731	1.6	25	Main-stem
M4	25.2	4.0	**678**	5.9	34	Partial
M5	21.8	2.6	606	4.3	54	Partial
M6	25.0	1.9	**678**	2.8	33	Partial
M7	24.0	4.2	340	12.4	53	Minimal
M8	32.9	3.5	**678**	5.2	43	Minimal
M9	25.6	3.6	643	5.6	52	Partial
M10	33.7	2.2	934	2.4	44	Partial
Mean	**24.9**	**2.8**	**678**	**4.7**	**42**	
Standard deviation	**7.0**	**0.9**	**144**	**2.9**	**12**	

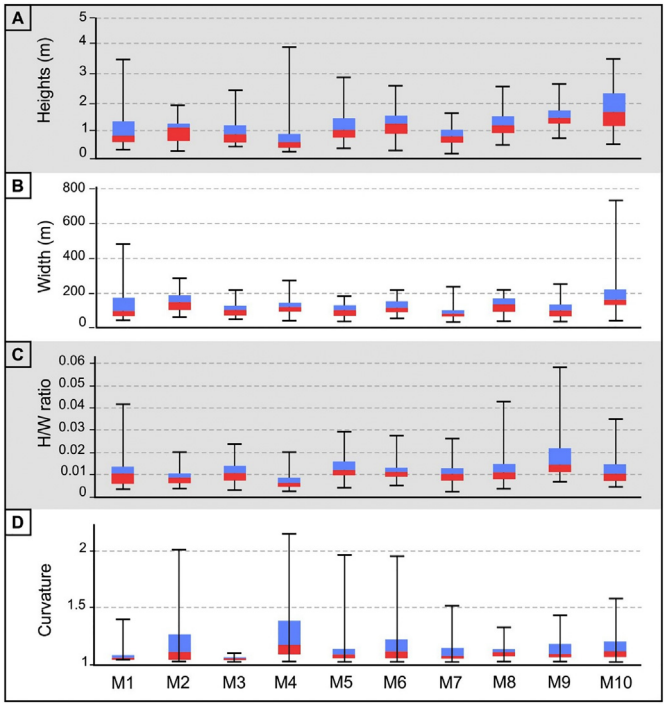

Fig. 6. Geomorphological attributes of scroll bar topography in 10 meander bends of the Mississippi River, showing range, 25th percentile (red box) and 75th percentile (blue box), and median. (A) Heights of scrolls relative to the point bar complex surface; (B) widths of scrolls; (C) height-to-width ratio of scrolls; and (D) curvature of scrolls.

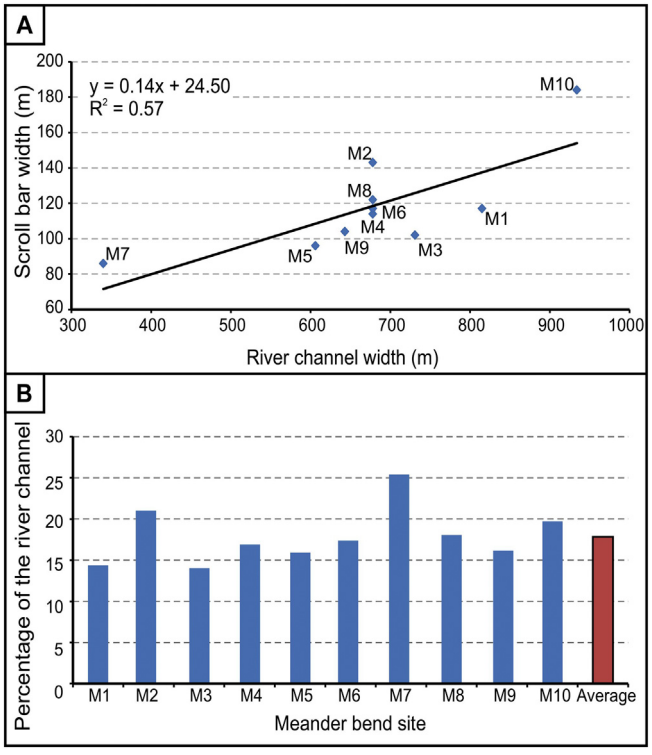

Fig. 7. (A) The relationship between scroll bar width (m) vs. the adjacent river channel width (m) for ten meander bends on the Mississippi floodplain; and (B) how scroll bar widths relate to the adjacent river channel per site and on average. Note that the variations for M4, M7, M8 and M2 in A are likely because these bends using a substitute average river channel width rather than the true river channel width, as a result of these channels having been filled in and the formative channel no longer obvious.

shown by the gradient of the linear equation in Fig. 7A. The results shown in Fig. 7A and B suggest a weak relationship between the width of scrolls and the width of the adjacent formative river channel.

The height-to-width ratio (H/W, Fig. 6C) of scrolls gives an indication of elevation forms; large values are representative of tall and narrow scrolls. On average, height-to-width ratios are low, indicating short and wide scrolls; but values do not exceed 0.06 and are on average 0.01.

Unlike the previous geomorphological attributes, the curvature of scrolls (Fig. 6D) shows much greater variability between meander bends, with much larger ranges compared to the quartiles and means. On average, scroll curvature for all 10 meander bends is 1.1, which is close to a straight line. This is caused by truncation of scrolls by the migrating river channel so that the curvature of preserved scroll remnants is reduced. However, bends such as M4, M5, M6, and M2 show values up to and exceeding 2, which indicates a more rounded scroll planform (Fig. 6D). The topography of scrolls that are preserved on the floodplain is not only dictated by the initial deposition of sediment but by the subsequent reworking of the channel as well. The basic geomorphological

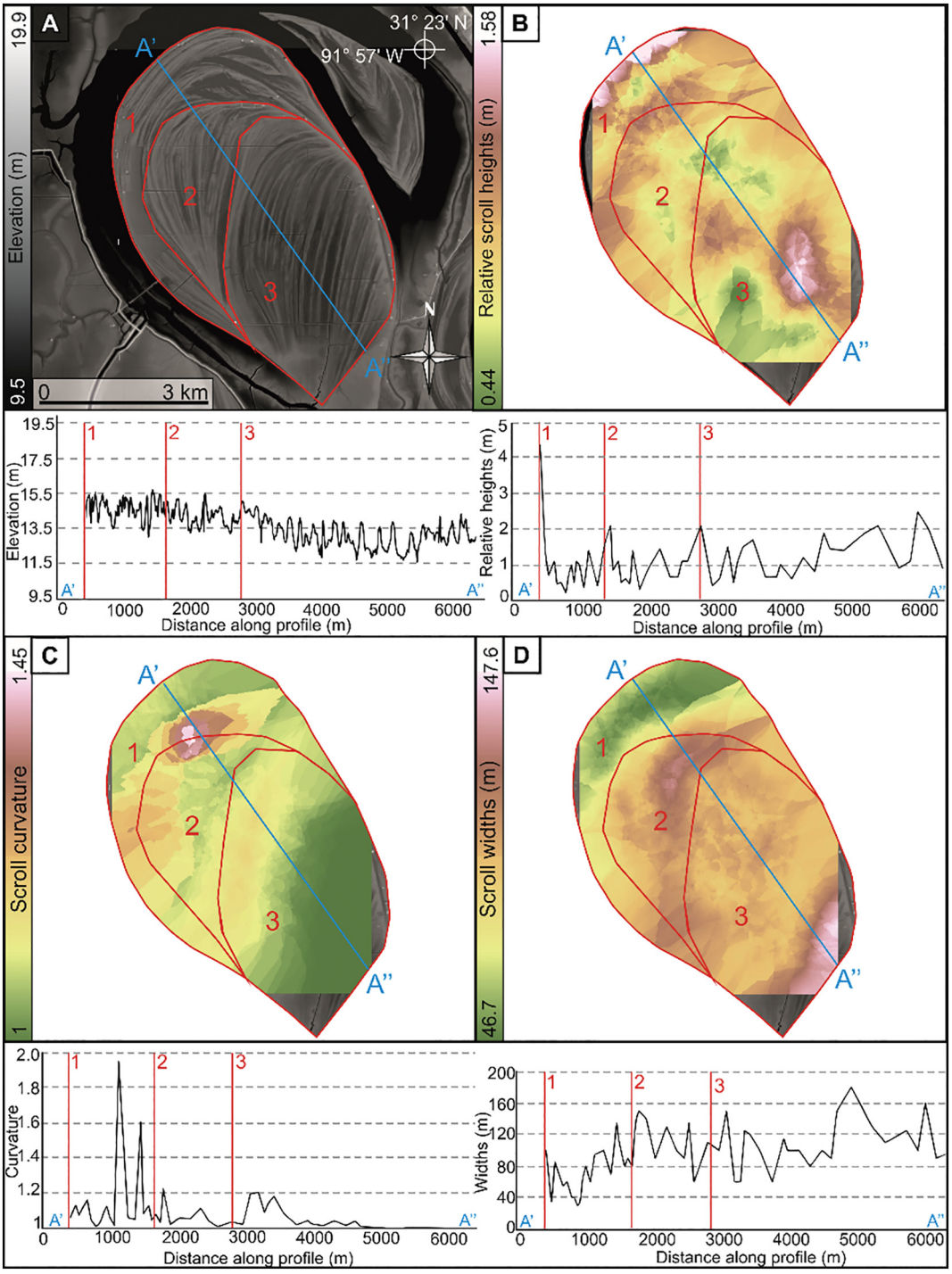

Fig. 8. Interpolation of scroll bar geometry to reveal the spatial distribution of scroll attributes and cross profiles through the interpolated data. Red lines and numbers depict the different depositional package boundaries. (A) DEM of meander bend 5 (M5) showing the different depositional packages and a profile line A′ to A″ of topography; (B) relative heights of scrolls (m); (C) curvature; and (D) widths of scrolls (m).

results summarised here indicate that the attributes of scrolls have inter- and intrascroll variability. The intra-scroll variability indicates a varied history of deposition and erosion during the evolution of each point bar.

4.3. Interpolation of scroll bar characteristics

Interpolating the data via Kriging 'smooths' the data across the point bar and reveals the general spatial distribution of scroll attributes. The following data analysis focuses on the relative heights of scrolls to the point bar surface, curvatures, and widths for the 10 study bends of the Mississippi River floodplain. Fig. 8 shows an example of the outputs for meander bend M5 created by the interpolation process before normalisation was implemented. Scroll heights are greatest at depositional package boundaries and then decrease until the next package boundary. Curvature is greatest at the boundaries of depositional packages (Fig. 8C), with an isolated spike of very high curvatures. Widths are narrowest close to the river channel with variations between depositional packages (Fig. 8D).

Normalising the data gives all attributes an equal range for all study sites, which supports a direct comparison between sites with scale independence. In this instance, the normalised data show the heights, widths, and curvatures of scrolls normalised to a scale of 0 to 1. The following data have been presented in Fig. 9 to show the interpolated data cropped within the scroll ridges themselves.

4.3.1. Relative scroll bar heights

Point bar complexes display considerable internal variability in relation to scroll heights, from tens of centimetres to 3 m; the distribution of these variations is nonuniform on a point bar surface. The 10 sites described show that relative scroll heights are greatest close to the current river channel and at the boundaries of depositional packages. This trend could be attributed to overbank sedimentation 'smoothing' older ridges to reduce their *relative* heights by the infilling of the adjacent swales. Sedimentation in depressions over time reduces the amplitude of positive and negative topographic features (Dunne and Aalto, 2013; Lewin et al., 2016). Higher sedimentation rates are found closer to the river channel (Walling and He, 1998); so with this infilling, relative relief will decrease over time.

The bends with the most undisturbed growth history (such as bends M3, M5 and M9) show most clearly the trend of scroll height decreasing away from the channel. These bends appear to have extended laterally in roughly the same direction, giving similar scroll orientations throughout their growth history. Bends with more complicated and variable growth histories - such as bends M10, M6, and M7 with their several depositional packages - display less obvious trends in scroll heights. These bends show more abrupt changes in scroll orientation between

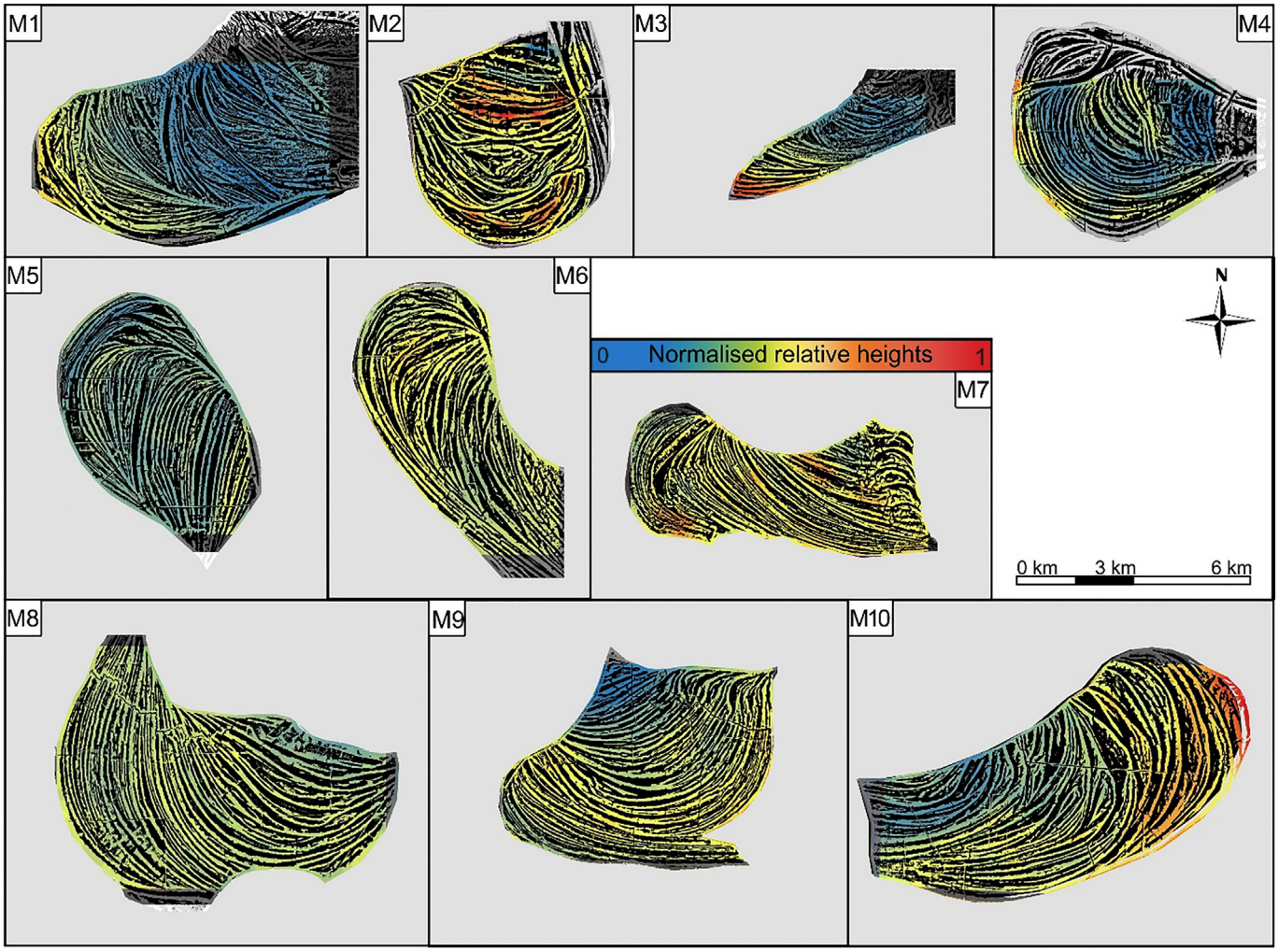

Fig. 9. Normalised interpolated relative scroll height data were cropped to produce a segmented scroll ridge image for better visualisation of geometric variations. Heights have been normalised to the dynamic range of each data-set to give values from 0 to 1; represented as a blue to red sequence. Black indicates swales between scroll ridges. These images were produced by the method of Automatic Local Thresholding (ALT), see text.

depositional packages, exhibiting not only lateral extension but also PBC rotation and truncation of scroll. This more complicated growth history has resulted in more spatially variable sedimentation processes caused by the reworking of the point bar surface and changing meander dynamics.

Relative scroll heights display nonuniformity on a point bar surface; but when compared to other point bars for the same river, relative scroll heights exhibit significant heterogeneity. This demonstrates that PBCs have dynamic intravariations in heights and that the local conditions are important in determining meander growth (and subsequently point bar formation and preservation). Scrolls are therefore, nonuniform in planform and size for the Mississippi River. A multimodal set of processes contributes to the formation of these landforms, including the channel geometry at time of deposition, later truncation by the migrating river channel, and the magnitudes of flood inundation.

4.4. Periodicity of scroll bars

To investigate scroll periodicity, a Fourier transform was implemented to present a spatial frequency power spectrum for each site. The 10 study sites of the Mississippi were analysed, investigating internal changes in scroll period in relation to point bar dynamics, and this was later extended to other rivers.

4.4.1. Mississippi scroll bar periodicity variations

The periodicity of scroll was determined for each depositional package per point bar complex (PBC). Each spatial frequency power spectrum (see Fig. 5 earlier) showed distinctive spikes that represent a dominant spatial frequency, which was then converted into periods for the following analysis.

The mean period of scrolls for the Mississippi River is 167 m, ranging from around 150 to 190 m, ridge top to ridge top. The bar charts in Fig. 10 show a variation between bends and within depositional packages within a bend. The dominant trend is that the farther away from the channel the spacing between scrolls increases (Fig. 10).

4.5. Scroll bar periodicity and river channel width for a range of rivers

A range of rivers, incorporating different river sizes and biogeomorphological settings, was further investigated; and a sample of point bar complexes from each was processed to determine their periodicity characteristics (Fig. 11 and listed in Table 4). The rivers chosen were primarily meandering, or at least ones with prominent meandering sections. However, by necessity, inclusion had to be determined by DEM data availability. If high-resolution LiDAR data were available, relatively small rivers could also be included. Where LiDAR was not available, coarser resolution data products had to be used including SRTM and ASTER global DEM VR2. This only gives satisfactory

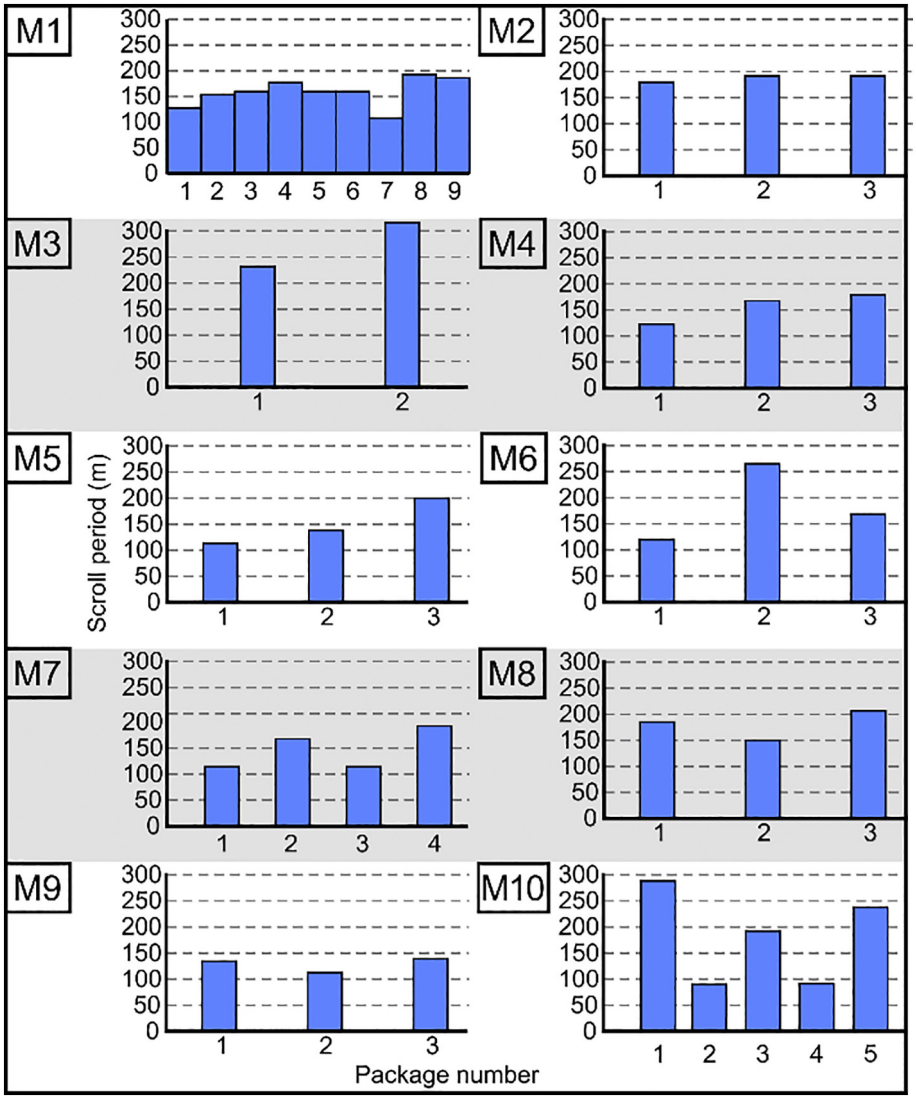

Fig. 10. Scroll period for each depositional package (DP) within ten different point bar complexes on the Mississippi River package numbers increase away from the adjacent river channel.

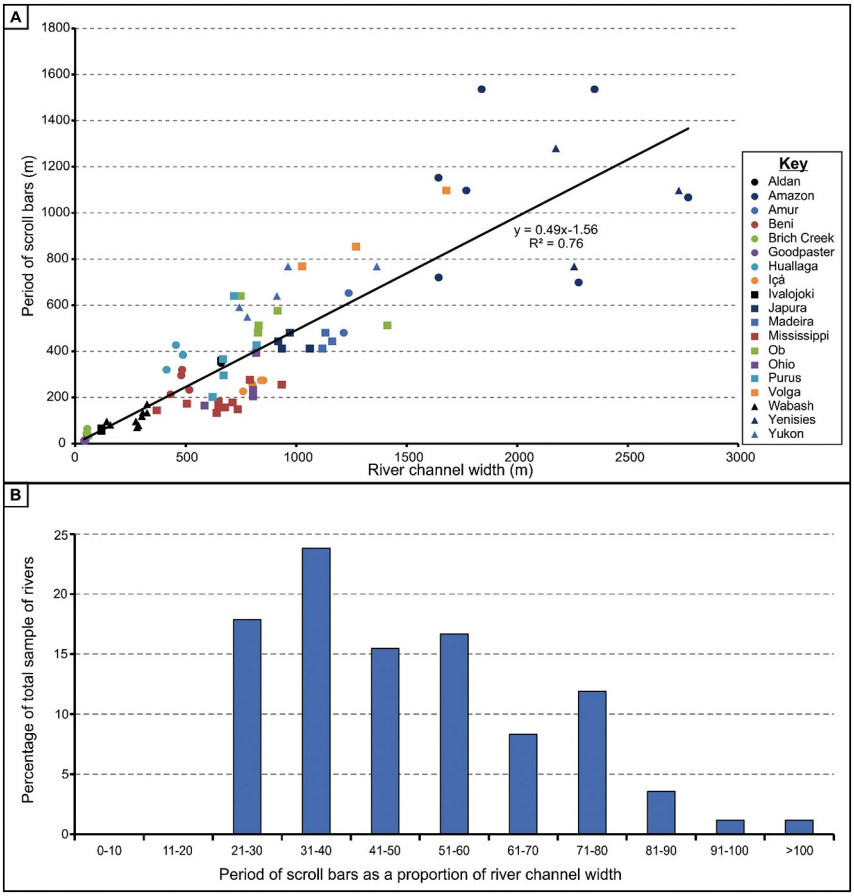

Fig. 11. (A) Relationship between the period of scroll bars and the adjacent river channel for 19 different rivers. A selection of meander bends was chosen per river, and the associated scroll bars were processed via the Fourier transform. (B) Histogram showing the spacing of scroll bars and the percentage of the river channel width the spacing is equal to, for the 19 rivers included in this study.

results on larger rivers because of the lower resolution (30-m spatial resolution).

The results presented in Fig. 11A show a strong positive linear relationship ($R^2 = 0.76$; p value ≤ 0.001) between the period of scrolls and the width of the adjacent river channel. This relationship is observed in a large range of rivers, from those with channels widths of 40 m to those with channels up to 2.4 km wide. Rivers were sourced from a range of climatic regions from high-latitude tundra to tropical forests. If the smaller river data are omitted, the relationship reduced to an R^2 of 0.66, though the gradient stays much the same at 0.50. Removing points derived from LiDAR only does not significantly reduce the relationship shown (R^2 of 0.65) but does reduce the gradient to 0.45. Fig. 11A demonstrates an overall relationship between scroll spacing and channel width, but an individual river may vary from this trend. For example, the Mississippi River data (Fig. 11A, red squares) plot below the trend line, with the periodicity of scrolls on average being 25% of the river channel as also shown in experimental work by van de Lageweg et al. (2014).

These data suggest that the spacing between individual scrolls is linked intrinsically with the width of the river channel as van de Lageweg et al. (2014) suggested from model studies. The period of scrolls/point bar deposits is linked to changes in macrochannel dynamics and processes. This close association with the river channel can be linked to equilibrium channel-width theories (Parker 1978a, 1978b); the maintenance of the channel width drives the deposition of new scrolls.

Fig. 11B shows the frequency distribution of data from all 19 rivers included in the extended study. There is no scroll spacing lower than 21% of the channel, and the distribution overall has a positive skew. This suggests that rivers migrate a minimum threshold distance before a scroll will form. The maximum values, representing the farthest a channel will migrate before a new scroll will form, are widely dispersed. A small minority of rivers migrate as much as a full river channel width

Table 4
Locations and attributes of rivers included in scroll periodicity investigation, ordered by annual average discharge; no gauge data was found for Brich Creek USA.

River name	Location of river	Annual average discharge (m^3/s)	Mean channel width (m)	Mean scroll spacing (m)	Data source
Amazon	Brazil	175,000	2042	1115	SRTM
Madeira	Brazil	24,852	1138	445	SRTM
Yenisei	Russia	19,600	2388	1048	ASTER
Mississippi	USA	16,792	665	180	LiDAR (5 m)
Japurá	Brazil	13,557	972	436	SRTM
Amur	Russian Far East	11,400	1226	566	ASTER
Purus	Brazil	10,400	701	386	SRTM
Ob	Russia	10,300	1069	544	SRTM/ASTER
Beni	Bolivia	8600	478	265	SRTM
Volga	Russia	8060	1326	906	ASTER
Ohio	USA	7957	753	249	LiDAR (1 m)
Içá	Peru	7502	814	258	SRTM
Yukon	USA	6368	953	663	LiDAR (3 m)
Aldan	Eastern Siberia	5060	660	357	ASTER
Huallaga	Peru	2900	453	377	SRTM
Wabash	USA	315	267	109	LiDAR (1 m)
Ivalojoki	Finland	39	119	60	LiDAR (2 m)
Goodpaster	USA	14	44	13	LiDAR (1 m)
Brich Creek	USA	NA	55	43	LiDAR (1 m)

before a scroll is formed. Most data fall within 20–60% of the width range of the river channel, so roughly equivalent to a quarter to a half of the river channel. This supports the view of a predictive rule for the relationship between scrolls and river channel width.

5. Discussion and conclusions

The geometric characteristics of 10 large point bars on the Lower Mississippi River have been quantified. The techniques developed on the Mississippi were then extended to investigate 19 other river sites. Analyses of the Mississippi were based on LiDAR-derived bare-earth DEMs and in other locations, for larger rivers, of the best available DEMs.

Point bar depositional features can be divided hierarchically into an individual scroll (S), depositional package (DP), and point bar complex (PBC). Standardised metrics have been devised for scroll widths, lengths, and heights. Analyses were then undertaken of relationships between them, of variations across PBCs, and between the dimensions of point bars and the adjacent river.

This work confirms previous model and theoretical conclusions concerning scroll spacing as based on different styles of investigation (Nanson, 1980; van de Lageweg et al., 2014) with scroll spacing approximating to 50% of river channel width ($R^2 = 0.76$). Hickin and Nanson (1975) showed that the periodicity of ridges is inversely related to channel migration rate and floodplain formation, whilst sedimentation rates are correlated with distance from channel and the density of floodplain vegetation. Spacing of scrolls for the Mississippi River decreases with increasing curvature, and this decrease in spacing is also seen in scrolls closest to the river channel, which is consistent with Hickin and Nanson's (1975) work presented above. The large river results demonstrated in this paper show that scroll width and periodicity for the Mississippi River are strongly connected to river channel width, highlighting the key link between processes and form. These results appear to be scale independent (Fig. 11), with rivers from a range of sizes adhering close to this relationship.

However, between and within point bar complexes have significant variations, especially when multiple depositional packages have evolving curvatures during bar growth. Relative heights, widths of the positive scroll element, and scroll curvatures are all different from one bend to another. Konsoer et al. (2016) showed that in large meandering rivers the erosion-resistance properties of banks and floodplains can vary substantially, laterally and vertically, over relatively short distances. Such variations in erosional properties of the bank and floodplain could account for the differences shown in scroll development and morphology. These differences for the Mississippi River become more pronounced at terminating boundaries because of a discontinuity of the deposition of sediments (Pietsch et al., 2015), which is associated with changes in the dynamics of meander bend development. Engel and Rhoads (2016) showed how the erosional characteristics of different lobes within compound meander bends increases the morphological complexity of the bend. This is reflected by bends on the Mississippi that appear to have undisturbed growth histories. These show more straightforward relative height decrease away from active channels, compared to more complex bends. This can be attributed to overbank sedimentation and subsequent smoothing of topography.

Scrolls are often truncated at the up- and downstream sections of the point bar so that the curvature preserved on the point bar surface is not indicative of the curvature at the time of deposition. This is shown by scrolls having an average curvature of 1.1 on the Mississippi River floodplain. This is important when interpreting preserved point bar deposits and reconstructing ancient meander bend morphodynamics. Evidence of this truncation of point bars is common; within a meander belt there is often evidence of truncated rotation, gradual rotation, and consistent expansion (Durkin et al., 2017). This is often caused by changes in the upstream channel geometry having a knock on effect on the accretion direction of the downstream bend.

Geometric analysis alone cannot reveal the physical processes or numerical timescales for point bar development, but dimensional analysis is useful in providing modern analogues to help constrain models of ancient geometry complexes that now are associated with hydrocarbon resource extraction. In such applications, the local geometry of coarser and finer sedimentary units can be critical for hydrocarbon yield (Nardin et al., 2013). Further work is still required to relate preserved point bar relief of large rivers to individual loop morphologies and dynamics (Ghinassi et al., 2016). Analysis of Holocene sequences of bend migration (Hudson and Kesel, 2000; Rodnight et al., 2005; Kasvi et al., 2017) can help give a temporal framework for scroll bar reworking and thus relate observations of modern process to preserved form.

Acknowledgements

Robert Strick would like to thank the Natural Environment Research Council for a PhD Studentship (NE/K501281/1) that funded the work herein. Phil Ashworth thanks the UK Natural Environment Research Council (NERC) for grant NE/E016022/1 that provided the early stimulus for discussions with colleagues on large river dynamics. We thank two anonymous referees and the editor for their helpful comments that improved the clarity of this paper.

References

Allen, J.R.L., 1965. A review of the origin and character of recent alluvial sediments. Sedimentology 5:89–191. https://doi.org/10.1111/j.1365-3091.1965.tb01561.x.
Ashworth, P.J., Lewin, J., 2012. How do big rivers come to be different? Earth Sci. Rev. 114: 84–107. https://doi.org/10.1016/j.earscirev.2012.05.003.
Aufdenkampe, A.L., Mayorga, E., Raymond, P.A., Melack, J.M., Doney, S.C., Alin, S.R., Aalto, R.E., Yoo, K., 2011. Riverine coupling of biogeochemical cycles between land, oceans and atmosphere. Ecol. Environ. 9:53–60. https://doi.org/10.1890/100014.
Autin, W.J., Burns, S.F., Miller, B.J., Saucier, R.T., Snead, J.I., 1991. Quaternary geology of the Lower Mississippi Valley. In: Morrison, R.B. (Ed.), Quaternary Nonglacial Geology: Conterminous. US Geological Society of America, Boulder, CO, pp. 547–582.
Biedenharn, D.S., Thorne, C.R., 1994. Magnitude-frequency analysis of sediment transport in the Lower Mississippi River. Regul. Rivers Res. Manag. 9:237–251. https://doi.org/10.1002/rrr.3450090405.
Blanckaert, K., de Vriend, H.J., 2010. Meander dynamics: a nonlinear model without curvature restrictions for flow in open-channel bends. J. Geophys. Res. 115:79–93. https://doi.org/10.1029/2009JF001301.
Carling, P., Jansen, J., Meshkova, L., 2013. Multichannel rivers: their definition and classification. Earth Surf. Process. Landf. 39:26–37. https://doi.org/10.1002/esp.3419.
Chen, D., Duan, J.D., 2006. Simulating sine-generated meandering channel evolution with an analytical model. J. Hydraul. Res. 44, 363–373.
Day, G., Dietrich, W.E., Rowland, J.C., Marshall, A., 2008. The depositional web on the floodplain of the Fly River, Papua New Guinea. J. Geophys. Res. 113. https://doi.org/10.1029/2006JF000622.
van Dijk, W.M., van de Lageweg, W.I., Kleinhans, M.G., 2013. Formation of a cohesive floodplain in a dynamic experimental meandering river. Earth Surf. Process. Landf. 38:1550–1565. https://doi.org/10.1002/esp.3400.
Dunne, T., Aalto, R.E., 2013. Large river floodplains. In: Shroder, J.F. (Ed.), Treatise on Geomorphology. vol. 9. Academic Press, San Diego, CA:pp. 645–678. https://doi.org/10.1016/B978-0-12-374739-6.00258-X.
Durkin, P.R., Hubbard, S.M., Boyd, R.L., Leckie, D.A., 2015. Stratigraphic expression of Intra-point-bar erosion and rotation. J. Sediment. Res. 85 1527-1404. https://doi.org/10.2110/jsr.2015.78.
Durkin, P.R., Boyd, R.L., Hubbard, S.M., Shultz, A.W., Blum, M.D., 2017. Three-dimensional reconstruction of meander-belt evolution, Cretaceous McMurray formation, Alberta Foreland Basin, Canada. J. Sediment. Res. 87:1075–1099. https://doi.org/10.2110/jsr.2017.59.
Engel, F.L., Rhoads, B.L., 2016. Three-dimensional flow structure and patterns of bed shear stress in an evolving compound meander bend. Earth Surf. Land. Proc. 41 (9): 1211–1226. https://doi.org/10.1002/esp.3895.
Fisk, H.N., 1944. Geological Investigation of the Alluvial Valley of the Lower Mississippi River. U.S. Army Corps Eng. Waterways Exp. Sta, Vicksburg, Mississippi.
Fisk, H.N., 1947. Fine-Grained Alluvial Deposits and Their Effects Upon Mississippi River Activity. Vicksburg, Mississippi River Commission.
Ghinassi, M., Ielpi, A., Aldinucci, M., Fustic, M., 2016. Downstream-migrating fluvial point bars in the rock record. Sediment. Geol. 334:66–96. https://doi.org/10.1016/j.sedgeo.2016.01.005.
Gouw, M.J.P., Autin, W.J., 2008. Alluvial architecture of the Holocene Lower Mississippi Valley (U.S.A.) and a comparison with the Rhine Meuse delta (The Netherlands). Sediment. Geol.:106–121 https://doi.org/10.1016/j.sedgeo.2008.01.003.
Gu, L., Zhang, S., He, L., Chen, D., Blanckaert, K., Ottevanger, W., Zhang, Y., 2016. Modelling flow pattern and evolution of meandering channels with a nonlinear model. Water 8: 418. https://doi.org/10.3390/w8100418.
Gupta, A., 2007. Large Rivers: Geomorphology and Management. Wiley, England (ISBN: 978-0-470-84987-3).

Happ, S.C., Rittenhouse, G., Dobson, G.C., 1940. Some Principles of Accelerated Stream and Valley Sedimentation. U S. Department of Agriculture Technology Bulletin:p. 695 https://doi.org/10.1177/0309133308091947.
Harmar, O.P., Clifford, N.J., 2006. Planform dynamics of the Lower Mississippi River. Earth Surf. Process. Landf. 7:825–843. https://doi.org/10.1002/esp.1294.
Hess, L.L., Melack, J.M., Novo, E.M.L.M., Barbosa, C.C.F., Gastil, M., 2003. Dual-season mapping of wetland inundation and vegetation for the central Amazon basin. Remote Sens. Environ. 87:404–428. https://doi.org/10.1016/j.rse.2003.04.001.
Hickin, E.J., 1974. The development of meanders in natural river-channel. Am. J. Sci. 274: 414–442. https://doi.org/10.2475/ajs.274.4.414.
Hickin, E.J., Nanson, G.C., 1975. The character of channel migration on the Beatton river, northeast British Columbia, Canada. Geol. Soc. Am. Bull. 86:487–494. https://doi.org/10.1130/0016-7606(1975)86<487:TCOCMO>2.0.CO;2.
Hooke, J.M., 2007. Complexity, self-organisation and variation in behaviour in meandering rivers. Geomorphology 91 (3):236–258. https://doi.org/10.1016/j.geomorph.2007.04.021.
Hooke, J.M., Harvey, A.M., 1983. Meander changes in relation to bend morphology and secondary flows. In: Collinson, J., Lewin, J. (Eds.), Modern and Ancient Fluvial Systems. International Association of Sediment Special Publication:pp. 121–132 https://doi.org/10.1002/9781444303773.ch9.
Hudson, P.F., Kesel, R.H., 2000. Channel migration and meander-bend curvature in the Lower Mississippi River prior to major human modification. Geology 28 (6): 531–534. https://doi.org/10.1130/0091-7613(2000).
Ikeda, S., Parker, G., Sawai, K., 1981. Bend theory of river meanders. Part 1. Linear development. J. Fluid Mech. 112:363–377. https://doi.org/10.1017/S0022112081000451.
Jackson, R.G., 1976. Largescale ripples of the lower Wabash River. Sedimentology 5: 593–623. https://doi.org/10.1111/j.1365-3091.1976.tb00097.x.
Kasvi, E., Laamanen, L., Lotsari, E., Alho, P., 2017. Flow patterns and morphological changes in a sandy meander bend during a flood-spatially and temporally intensive ADCP measurement approach. Water 9:106. https://doi.org/10.3390/w9020106.
Knox, J.C., 2007. In: Gupta, A. (Ed.), The Mississippi River System, in Large Rivers: Geomorphology and Management. John Wiley & Sons, Ltd, Chichester, UK https://doi.org/10.1002/9780470723722.ch9.
Knox, R.L., Latrubesse, E.M., 2016. A geomorphic approach to the analysis of bedload and bed morphology of the Lower Mississippi River near the Old River Control Structure. Geomorphology 268:35–47. https://doi.org/10.1016/j.geomorph.2016.05.034.
Konsoer, K.M., Rhoads, B.L., Langendoen, E.J., Best, J.L., Ursic, M.E., Abad, J.D., Garcia, M.H., 2016. Spatial variability in bank resistance to erosion on a large meandering, mixed bedrock-alluvial river. Geomorphology 252:80–97. https://doi.org/10.1016/j.geomorph.2015.08.002.
van de Lageweg, W.I., van Dijk, W.M., Baar, A.W., Rutten, J., Kleinhans, M.G., 2014. Bank pull or bar push: what drives scroll-bar formation in meandering rivers? Geology 85:1238–1257. https://doi.org/10.1130/G35192.1.
Landini, G., 2016. Auto Local Threshold (ImageJ). Accessed:. https://github.com/fiji/Auto_Threshold/blob/master/src/main/java/fiji/threshold/Auto_Local_Threshold.java.
Lanzoni, S., Seminara, G., 2006. On the nature of meander instability. J. Geophys. Res. 111, F04006. https://doi.org/10.1029/2005JF000416.
Latrubesse, E.M., 2008. Patterns of anabranching channels: the ultimate end-member adjustment of mega rivers. Geomorphology 101:130–145. https://doi.org/10.1016/j.geomorph.2008.05.035.
Latrubesse, E.M., 2015. Large rivers, megafans and other quaternary avulsive fluvial systems: a potential 'who's who' in the geological record. Earth Sci. Rev. 146:1–30. https://doi.org/10.1016/j.earscirev.2015.03.004.
Lazarus, E.D., Constantine, J.A., 2013. Generic theory for channel sinuosity. Proc. Natl. Acad. Sci. U. S. A.. 110:pp. 8447–8452. https://doi.org/10.1073/pnas.1214074110
Leclerc, R.F., Hickin, E.J., 1997. The internal structure of scrolled floodplain deposits based on ground-penertrating radar, North Thompson River, British Columbia. Geomorphology 21:17–38. https://doi.org/10.1016/S0169-555X(97)00037-8.
Leopold, L.B., Wolman, M.G., Miller, J.P., 1964. Fluvial Processes in Geomorphology. W. H. Freeman Co., San Francisco (Pages 317).
Lewin, J., Ashworth, P.J., 2014a. Defining large river channel patterns: alluvial exchange and plurality. Geomorphology 215:83–98. https://doi.org/10.1016/j.geomorph.2013.02.024.
Lewin, J., Ashworth, P.J., 2014b. The negative relief of large river floodplains. Earth Sci. Rev. 129:1–23. https://doi.org/10.1016/j.earscirev.2013.10.014.
Lewin, J., Ashworth, P.J., Strick, R.J.P., 2016. Spillage sedimentation on large river floodplains. Earth Surf. Process. Landf. https://doi.org/10.1002/esp.3996.
Luchi, R., Bolla Pittaluga, M., Seminara, G., 2010. Morphodynamic response of meandering channels to width variations. American Geophysical Union, Fall Meeting 2010 (abstract id. EP51C-0563).
Martinius, A.W., Fustic, M., Garner, D.L., Jablonski, B.V.J., Strobl, R.S., MacEachen, J.A., Dashtgard, S.E., 2017. Reservoir characterization and multiscale heterogeneity modelling of inclined heterolithic strata for bitumen-production forecasting, McMurray Formation, Corner, Alberta, Canada. Mar. Pet. Geol. 82:336–361. https://doi.org/10.1016/j.marpetgeo.2017.02.003.
Mertes, L.A.K., 1997. Documentation and significance of the perirheic zone on inundated floodplains. Water Resour. Res. 33:1749–1762. https://doi.org/10.1029/97WR00658.
Mertes, L.A.K., Dunne, T., Martinelli, L.A., 1996. Channel-floodplain geomorphology along the Solimões - Amazon River, Brazil. Geol. Soc. Am. Bull. 108:1089–1107. https://doi.org/10.1130/00167606(1996)108<1089:CFGATS>2.3.CO;2.
Moreton, D., Carter, J., 2015. Characterizing alluvial architecture of point bars within the McMurray Formation, Alberta, Canada, for improved bitumen resource prediction and recovery. In: Best, J. (2015) Fluvial-Tidal Sedimentology. Dev. Sedimentol. 68: 529–559. https://doi.org/10.1016/B978-0-444-63529-7.00016-X.
Nanson, G.C., 1980. Point bar and floodplain formation of the meandering Beatton River, northeastern British Columbia, Canada. Sedimentology 27:3–29. https://doi.org/10.1111/j.1365-3091.1980.tb01155.x.
Nardin, T.R., Feldman, H.R., Carter, B.J., 2013. Stratigraphic architecture of a large-scale point-bar complex in the McMurray Formation: Syncrude's Mildred Lake Mine, Alberta, Canada. In: F., J. (Ed.), Chapter 9 IN Studies in Geology.
O'Loughlin, F.O., Trigg, M.A., Schumann, G.J.-P., Bates, P.D., 2013. Hydraulic characterisation of the middle reach of the Congo River. Water Resour. Res. 49:5059–5070. https://doi.org/10.1002/wrcr.20398.
Parker, G., 1978a. Self-formed straight rivers with equilibrium banks and mobile bed, Part 1. The Sand-silt river. J. Fluid Mech. 89 (01):109–125. https://doi.org/10.1017/S0022112078002499.
Parker, G., 1978b. Self-formed straight rivers with equilibrium banks and mobile bed, part 2. The gravel river. J. Fluid Mech. 89:127–146. https://doi.org/10.1017/S0022112078002505.
Parker, G., Wilcock, P.R., Paola, C., Dietrich, W.E., Pitlick, J., 2007. Physical basis for quasi-universal relations describing bankfull hydraulic geometry of single-thread gravel bed rivers. J. Geophys. Res. 112. https://doi.org/10.1029/2006JF000549.
Parker, G., Shimizu, Y., Wilkerson, G.V., Eke, E.C., Abad, J.D., Lauer, J.W., Paola, C., Dietrich, W.E., Woller, V.R., 2011. A new framework for modelling the migration of meandering rivers. Earth Surf. Process. Landf. 36 (1):70–86. https://doi.org/10.1002/esp.2113.
Peakall, J., Ashworth, P.J., Best, J.L., 2007. Meander-bend evolution, alluvial architecture, and the role of cohesion in sinuous river channels: a flume study. J. Sediment. Res. 77:197–212. https://doi.org/10.2110/jsr.2007.017.
Pietsch, T.J., Brooks, A.P., Spencer, J., Oley, J.M., Borombovits, D., 2015. Age, distribution, and significance within a sediment budget, of in-channel depositional surfaces in the Normanby River, Queensland, Australia. Geomorphology 239:17–40. https://doi.org/10.1016/j.geomorph.2015.01.038.
Rodnight, H., Duller, G.A.T., Tooth, S., Wintle, A.G., 2005. Optical dating of a scroll-bar sequence on the Kilp River, South Africa, to derive the lateral migration rate of a meander bend. The Holocene 15:802–811. https://doi.org/10.1191/0959683605hl854ra.
Rozo, M.G., Nogueira, A.C.R., Truckenbrodt, W., 2012. The anastomosing pattern and the extensively distributed scroll bars in the middle Amazon River. Earth Surf. Process. Landf. 14:1471–1488. https://doi.org/10.1002/esp.3249.
Saucier, R.T., 1994. Geomorphology and Quaternary Geologic History of the Lower Mississippi Valley. U. S. Army Engineer Waterways Experiment Station, Vicksburg, Mississippi.
Schwenk, J., Lanzoni, S., Foufoula-Georgiou, E., 2015. The life of a meander bend: connecting shape and dynamics via analysis of a numerical model. J. Geophys. Res. Earth Surf. 120 (4):690–720. https://doi.org/10.1002/2014JF003252.
Sun, T., Meakin, P., Jøssang, T., Schwarz, K., 1996. A simulation model for meandering rivers. Water Resour. Res. 32 (9):2937–2954. https://doi.org/10.1029/96WR00998.
Trigg, M.A., Bates, P.D., Wilson, M.D., Schumann, G., Bauch, C., 2012. Floodplain channel morphology and networks of the middle Amazon River. Water Resour. Res. 48 (10). https://doi.org/10.1029/2012WR011888.
Trigg, M.A., Michaelides, K., Neal, J.C., Bates, P.D., 2014. Surface water connectivity dynamics of a large scale extreme flood. J. Hydrol. 505:138–149. https://doi.org/10.1016/j.jhydrol.2013.09.035.
Vermeulen, B., Hoitink, A.J.F., Zolezzi, G., Abad, J.D., Aalto, R., 2016. Multi-scale structure of meanders. Geophys. Res. Lett. 43 (7):3288–3297. https://doi.org/10.1002/2016GL068238.
Walling, D.E., He, Q., 1998. The spatial variability of overbank sedimentation on river floodplains. Geomorphology 24:209–223. https://doi.org/10.1016/S0169-555X(98)00017-8.
Zolezzi, G., Seminara, G., 2001. Downstream and upstream influence in river meandering. Part 1. General theory and application to overdeepening. J. Fluid Mech. 438:183–211. https://doi.org/10.1017/S002211200100427X.